Project Title:

Numerical study on the relationship of cardiovascular system and glomerular filtration rate

Name: Chang-Jin JI
Laboratory: Advanced center for computing and communications

1. Background and purpose

The partial occlusion of arteries due to stenotic obstruction is one of the most frequently occurring abnormalities in human body. Once an obstruction has developed, the flow of blood will be disturbed and hemodynamic factors must play an increasingly important role as the stenosis continues to develop [1]. For comprehensive studies on the systemic arterial tree based on the 1-D model [2, 3], it is necessary to model the pressure drop across the stenosis. Despite a number of experimental and numerical studies, it is nontrivial since the interplay among the geometry, the hydrodynamic nonlinearity and the unsteadiness gives rise to a complicated aspect.

Our focus is on the issue how to systematically model the relation between the pressure drop and the flow rate in terms of the stenosis severity and the convective momentum transport. We perform numerical simulations of simplified stenotic flows (Fig. 1) using a voxel-based simulator [4], and analyses based on Lorentz's reciprocal theorem [5]. We derive an identity accounting for the pressure drop mechanism [6], and demonstrate its validity for a preliminary computation of a steady flow.

2. Method

2.1. Lorentz reciprocal theorem

We call the solutions $\boldsymbol{u}$, p as the NS (Navier-Stokes) solutions. We also find solutions to the steady Stokes equation (involving no advection term) with the same fluid properties and boundary conditions Hereafter, a quantity with the superscript * stands for the Stokes flow solution. Let us consider the Lorentz reciprocal theorem [5]

$$(\nabla \boldsymbol{u}) : \boldsymbol{\sigma}^* = (\nabla \boldsymbol{u}^*) : \boldsymbol{\sigma}. \qquad (5)$$

Using no-slip condition on the wall and taking the volume integral of two sides of the equation.

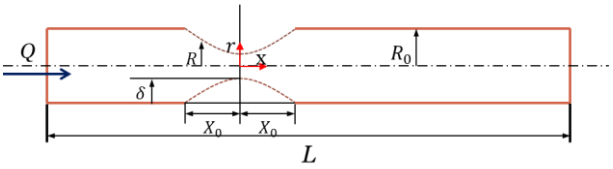

Fig. 1 Simplified geometric model for stenosis vessel. The shape function is: $\frac{R}{R_0} = 1 - \frac{\delta}{2R_0}\left(1 + \cos\frac{\pi x}{X_0}\right), \quad -X_0 \le x \le X_0$

Finally, we arrive at an identical relation

$$\Delta P Q^* = \Delta P^* Q - \int (u_i u_j D_{ij}{}^*) dV$$

$$-\frac{2}{Re}\left(\iint n_i u_j{}^* D_{ij}\, dS - \iint n_i u_j D_{ij}{}^*\, dS\right)_{\partial\Omega_{in} \,\&\, \partial\Omega_{out}}$$

$$+\left(\iint n_i (u_i u_j u_j{}^*)\, dS\right)_{\partial\Omega_{in} \,\&\, \partial\Omega_{out}}. \qquad (1)$$

Note that in the Stokes flow, the pressure drop ΔP^* is linear with respect to the flow rate Q^*. When ΔP^* is controlled to be $Q^* = Q$, the difference $\Delta P - \Delta P^*$ is determined from the spatial distribution of the velocity vectors $\boldsymbol{u}$, $\boldsymbol{u}^*$ as indicated in Eq. (8).

2.2 Lubrication

In the neighbourhood of any station x, the tube radius and the axial pressure gradient are approximately uniform with values $R(x)$ and $-G(x)$, the approximate expression for the axial velocity obtained by neglecting the inertia force (Poiseuille flow)

$$\Delta p = p_1 - p_2 = \frac{1}{Re}\frac{8Q}{\pi}\int_0^L R^{-4}\, dx \qquad (2)$$

3. Numerical results

We perform numerical simulations using a voxel-based simulator "V-FLOW VOF3D" [4], in which the vessel geometry is expressed using VOF and AOF functions on a Cartesian mesh. As schematically illustrated in Fig. 1, we consider a simplified geometric model for a stenosis vessel with $\delta = 0.5R_0$, $X_0 = 4R_0$, $L_1 = 2R_0$, and $L_2 = 10R_0$. The flow rate at the inlet for both the NS and Stokes flows is prescribed to be $Re = 500$, namely $Q^* = Q = 125\pi\mu R_0/\rho$. The pressure drops ΔP, ΔP^* are obtained as the simulation results.

A: distributions of streamwise velocity component (NS flow)

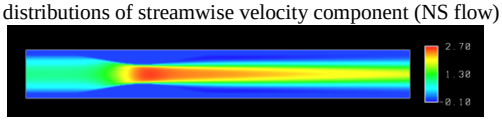

B: pressure distributions (NS flow)

C: distributions of streamwise velocity component (Stokes flow)

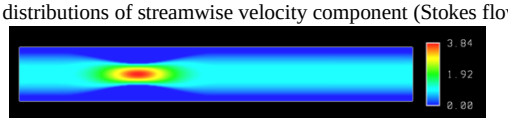

D: pressure distributions (Stokes flow)

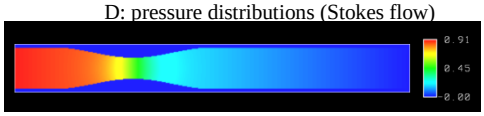

Fig. 2 The velocity and pressure distributions for the NS solutions (Eqs. (1), (2)) at Re = 500, and the Stokes ones (Eq. (4)).

3.1 Features of NS flow and Stokes flow

Fig. 2 visualizes the velocity and pressure distributions. In the Stokes flow, the velocity distribution (Fig. 2C) is almost symmetric with respect to the throat point, and the pressure (Fig. 2D) reduces monotonically in the downstream. By contrast, due to the enhanced inertia in the NS flow, the velocity (Fig. 2A) on the axis $r = 0$ behind the stenosis is obviously higher than that in front of the stenosis, and the pressure (Fig. 2B) reveals a non-monotonous profile with a local minimum in the stenosis region.

3.2 Validation of Lorentz reciprocal theorem and Lubrication theory

To make verification of Lorentz reciprocal theorem and Lubrication theory, we obtained the results when Re is equal to [1, 2, 5, 10, 20, 50, 100-1000] and

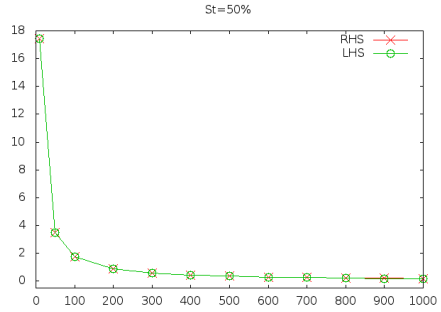

Fig.3 Validation of Lorentz reciprocal theorem

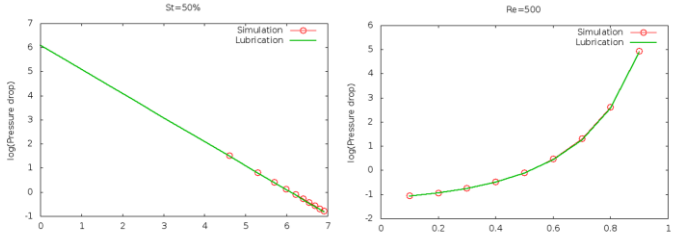

Fig.4 Validation of Lubrication theory

St (stenosis severity) is equal to [0.1, 0.2, …, 0.9], respectively, by using RICC. Fig. 3 shows the value of two sides in Eq. (1), which are numerically evaluated using the simulation results. The total value in the RHS is in good agreement with the LHS, indicating the consistency between Lorentz reciprocal theorem and the numerical simulation. Similarly, Fig.4 shows the verification result of Eq. (2). We can predict that the Lubrication theory can be applied to estimate the solution of Stokes flow in stenosis pipe.

4. Discussion and Conclusion

4-1 On the effect of inlet and outlet velocities

The third and fourth terms in the RHS of Eq. (8) are the contributions at the inlet and outlet boundaries. From Table1, the magnitude of the third term is negligibly smaller than other terms. The fourth term is non-negligible because the stenosis makes the velocity at the outlet larger than that at the inlet (see Fig. 2 A). However, if the pipe is long enough, the radial profiles of the streamwise velocity component at both the inlet and outlet may be regarded as parabolic, and thus the surface integrals over the inlet and outlet boundaries involved in the fourth term are likely to compensate each other. Therefore, the following relation may hold for a sufficiently long pipe:

$$\Delta P = \Delta P^* + \frac{1}{Q}\int\left(-u_i u_j D_{ij}{}^*\right)dV. \quad (3)$$

Note that the Stokes flow solution ΔP^* is the lower bound for fixed Q [7]. Therefore, the second term in the RHS of Eq. (3) is guaranteed to be positive, and responsible for the extra pressure drop owing to the convective momentum transport.

4-2 On the effect of the directionality

The correlation $-u_i u_j D_{ij}{}^*$ is expressed as

$$-u_i u_j D_{ij}{}^* = \underbrace{-u_x{}^2 D_{xx}{}^*}_{(a)} \underbrace{-u_y{}^2 D_{yy}{}^* - u_z{}^2 D_{zz}{}^*}_{(b)}$$

$$\underbrace{-2u_x u_y D_{xy}{}^* - 2u_x u_z D_{xz}{}^*}_{(c)} \underbrace{-2u_y u_z D_{yz}{}^*}_{(d)} . \quad (10)$$

These six terms can be classified into four categories (a)–(d) in terms of the streamwise (x) and axis-normal (y, z) directions. Table 2 reports the contributions of the respective components to the pressure drop. From Table 2, the xx component (category (a)) is dominant for the increase in the pressure drop. Unlike the turbulent flow in a straight pipe, the xy and xz components (category (c)), which are generally related to the Reynolds shear stress and the turbulence kinetic-energy production, are negative, implying the drag reduction contribution. In the upstream and downstream regions from the throat, the strain rates $D_{xx}{}^*$ in the Stokes flow are negative and positive, respectively. The square velocity $u_x{}^2$ close to the axis $r = 0$ in the downstream region is higher than that in the upstream region (see Fig. 2A). Such an inertia effect leads to the positive integral value of $-u_x{}^2 D_{xx}{}^*$ over the whole fluid region, and thus is reflected on the drag increase.

Table 2 Contributions of each term in Eq. (10) to the pressure drop

xx	yy	zz	xy	xz	yz
0.7816	-7.65×10^{-4}	-7.65×10^{-4}	−0.2297	−0.2298	-1.12×10^{-3}

The identical relation (Eq. (8)) obtained from the Lorentz reciprocal theorem [5] was confirmed to connect the pressure drop-flow rate relation with the spatial velocity distribution, for which we can access several physical pictures based on e.g. lubrication, Re-expansion and boundary-layer theories. We will perform the analysis over a wider range of parameter space.

References

1) D. Young and F. Tsai: Flow characteristics in models of arterial stenoses – I. steady flow, J. Biomechanics, Vol. 6, pp.395-410, 1973.
2) N. Stergiopulos, D. Young and T. Rogge: Computer simulation of arterial flow with applications to arterial and aortic stenoses, J. Biomechanics, Vol. 25, pp.1477-1488, 1992.
3) F. Y. Liang, K. Fukasaku, H. Liu and S. Takagi: A Computational model study of the influence of the anatomy of the circle of Willis on cerebral hyperperfusion following carotid artery surgery, Biomedical Engineering Online, Vol. 10, 84, 2011.
4) S. Noda, K. Fukasaku, and R. Himeno: Blood flow simulator using medical images without mesh generation, IFMBE Proc. of World Congress on Medical Physics and Biomedical Engineering, pp. 36-40, 2006.
5) J. Happel and H. Brenner: Low Reynolds Number Hydrodynamics, Martinus Nijhoff Publishers, The Hague, Chap. 3, 1983.
6) M. Sbragaglia and K. Sugiyama: Boundary induced nonlinearities at small Reynolds numbers, Physica D, Vol. 228, pp.140-147, 2007.
7) K. Fukagata, K. Sugiyama and N. Kasagi: On the lower bound of net driving power in controlled duct flows, Physica D, Vol. 238, pp.1082-1086, 2009.

Fiscal Year 2012 List of Publications Resulting from the Use of RICC

[Publication]

[Proceedings, etc.]

Title of the presentation: On the modeling of pressure drop in stenotic flows.

proceedings name: Proceedings of National Committee for Theoretical and Applied Mechanics Japan.

Date: Mar. 8th 2013

Paper info. :
Chang-Jin Ji, Kazuyasu Sugiyama, Shigeho Noda, Ying He, Ryutaro Himeno, On the modeling of the pressure drop in stenotic flows, Proc. of 62nd National Congress of Theoretical and Applied Mechanics, (2013) No. 100188.

[Oral presentation at an international symposium]

[Others]